

Article

Pinostrobin and Tectochrysin Conquer Multidrug-Resistant Cancer Cells via Inhibiting P-Glycoprotein ATPase

I-Ting Wu ^{1,†}, Chan-Yen Kuo ^{2,†} , Ching-Hui Su ¹, Yu-Hsuan Lan ¹ and Chin-Chuan Hung ^{1,3,4,*} 

¹ Department of Pharmacy, China Medical University, No. 100, Sec. 1, Jingmao Rd., Beitun District, Taichung 406040, Taiwan

² Department of Research, Taipei Tzu Chi Hospital, Buddhist Tzu Chi Medical Foundation, New Taipei City 231405, Taiwan

³ Department of Pharmacy, China Medical University Hospital, No. 2, Yude Rd., North District, Taichung 404332, Taiwan

⁴ Department of Healthcare Administration, Asia University, 500, Lioufeng Rd., Wufeng, Taichung 41354, Taiwan

* Correspondence: cc0206hung@gmail.com

† These authors contributed equally to this work.

Abstract: Enhanced drug efflux through ATP-binding cassette transporters, particularly P-glycoprotein (P-gp), is a key mechanism underlying multidrug resistance (MDR). In the present study, we investigated the inhibitory effects of pinostrobin and tectochrysin on P-gp in MDR cancer cells and the underlying mechanisms. Fluorescence substrate efflux assays, multidrug resistance 1 (MDR1) shift assays, P-gp ATPase activity assays, Western blotting, and docking simulation were performed. The potential of the test compounds for MDR reversal and the associated molecular mechanisms were investigated through cell viability assay, cell cycle analysis, apoptosis assay, and further determining the combination index. Results demonstrated that pinostrobin and tectochrysin were not the substrates of P-gp, nor did they affect the expression of this transporter. Both compounds noncompetitively inhibited the efflux of rhodamine 123 and doxorubicin through P-gp. Furthermore, they resensitized MDR cancer cells to chemotherapeutic drugs, such as vincristine, paclitaxel, and docetaxel; thus, they exhibited strong MDR reversal effects. Our findings indicate that pinostrobin and tectochrysin are effective P-gp inhibitors and promising candidates for resensitizing MDR cancer cells.

Keywords: drug efflux; ATPase; pinostrobin; tectochrysin; Flavonoid; multidrug resistance; P-glycoprotein



check for updates

Citation: Wu, I.-T.; Kuo, C.-Y.; Su, C.-H.; Lan, Y.-H.; Hung, C.-C. Pinostrobin and Tectochrysin Conquer Multidrug-Resistant Cancer Cells via Inhibiting P-Glycoprotein ATPase. *Pharmaceuticals* **2023**, *16*, 205. <https://doi.org/10.3390/ph16020205>

Academic Editor: Monica Notarbartolo

Received: 28 November 2022

Revised: 19 January 2023

Accepted: 25 January 2023

Published: 29 January 2023



Copyright: © 2023 by the authors. Licensee MDPI, Basel, Switzerland. This article is an open access article distributed under the terms and conditions of the Creative Commons Attribution (CC BY) license (<https://creativecommons.org/licenses/by/4.0/>).

1. Introduction

Cancer is the primary reason for death worldwide. Although various options, such as surgery, radiation therapy, immunotherapy, and hormone therapy, can be used for treating cancer, chemotherapy remains the predominant treatment option. Multidrug resistance (MDR) is a major concern in chemotherapy. Numerous mechanisms underlie the development of MDR, such as enhanced DNA repair capacity, increased drug efflux, mutated drug targets, and uncontrolled cell cycles, etc. [1,2]. Among these mechanisms, enhanced drug efflux is a key process.

In the cell membrane, ATP-binding cassette (ABC) transporters, such as P-glycoprotein (P-gp/MDR1/ABCB1), breast cancer resistance protein (BCRP; ABCG2), and multidrug resistance-associated protein 1 (MRP1; ABCC1), regulate the absorption, distribution, and excretion of various compounds. High expression levels of ABC transporters on the surface of cancer cells may reduce chemotherapeutic drug penetration and intracellular concentration. For instance, P-gp is often expressed at high levels on the surface of endothelial cells, thus hindering the penetration of chemotherapeutic drugs. P-gp and BCRP efflux various anticancer agents that are structurally and functionally unrelated, such as taxanes,

vinca alkaloids, anthracyclines, colchicine, and mitoxantrone, thus reducing intracellular drug accumulation and drug efficacy. Many types of cancer express ABC transporters, such as colorectal cancer, liver cancer, acute myeloid (AML), and breast cancer. Approximately 35% of acute myeloid leukemia and 71% of relapsed breast cancer cases involve the overexpression of P-gp, leading to the failure of anticancer therapies [3–5]. Furthermore, chemotherapy failure may result from inflammation and tumor gene mutations [1,2].

Among phytochemicals, alkaloids are the most extensively studied secondary metabolites in the context of MDR [6]. Flavonoids, another important group of secondary metabolites, exhibit in vitro anti-inflammatory, antiviral, antiallergic, anticarcinogenic, antimutagenic, and osteogenetic activities. To date, various secondary metabolites, such as genistein, naringenin, and curcumin, have been reported to affect ABC transporters [7]. Pinostrobin (Figure 1a), a dietary bioflavonoid isolated from *Pinus strobus*, exhibits antiviral (against herpes simplex virus-1) and antibacterial (against *Helicobacter pylori*) activities. This bioflavonoid also exhibits anti-inflammatory activities, including the inhibition of the expression of tumor necrosis factor (TNF)- α , interleukin-1 β , cyclooxygenase (COX)I, and COXII [8]. Furthermore, pinostrobin inhibits the formation of focal and cell adhesions to reduce the migration of malignant breast epithelial cells [9]. This finding indicates that pinostrobin can be used to control the progression of advanced breast cancer. Previous studies have reported that this compound exhibits no substantial cytotoxicity in drug-sensitive and drug-resistant cell lines [8–11].

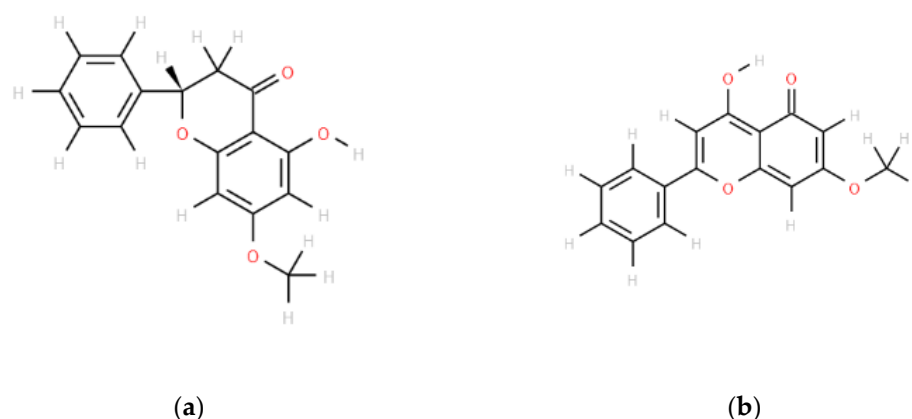


Figure 1. Structures of pinostrobin (a) and tectochrysin (b).

Tectochrysin (Figure 1b) is isolated from *Alpinia oxyphylla*. This compound exerts antiproliferative effects on human colorectal adenocarcinoma cells by inducing the expression of DR3, DR4, Fas, and proapoptotic proteins and inhibiting the activity of NF- κ B [12]. Tectochrysin alleviates A β 1–42-induced impairments of spatial learning and memory in mice, which indicates its therapeutic potential for Alzheimer’s disease [13]. The combination of tectochrysin with cetuximab inhibits epidermal growth factor receptor signaling to control the growth of cancer cells [14]. It is a potent inhibitor of ABCG2-mediated drug efflux [15].

The effects of pinostrobin and tectochrysin on MDR reversal and P-gp activity have been minimally explored in previous studies [15,16], but their mechanisms of action have not been investigated in depth. Therefore, in the present study, we assessed the effects of pinostrobin and tectochrysin on the expression and function of P-gp and its kinetics to elucidate the underlying molecular mechanisms. In addition, we investigated the efficacy of the combination of pinostrobin or tectochrysin with chemotherapeutic drugs in MDR cancer cells; for this, the potential of pinostrobin and tectochrysin for MDR reversal was evaluated.

2. Results

2.1. Inhibitory Effects of Pinostrobin and Tectochrysin on Efflux Function and Kinetic Mechanisms

To determine whether pinostrobin and tectochrysin affected the efflux function of human P-gp, we performed calcein-AM uptake assays. Calcein-AM, a nonfluorescent

compound, penetrates viable cells and is hydrolyzed by intracellular esterases to produce fluorescent calcein. Calcein is a substrate of P-gp; therefore, the inhibition of P-gp interferes with calcein efflux, which, in turn, prevents the accumulation fluorescent calcein in cells. As shown in Figure 2, the intensity of intracellular calcein fluorescence markedly increased with the increasing concentrations of pinostrobin and tectochrysin. Therefore, pinostrobin and tectochrysin may inhibit the efflux function of P-gp.

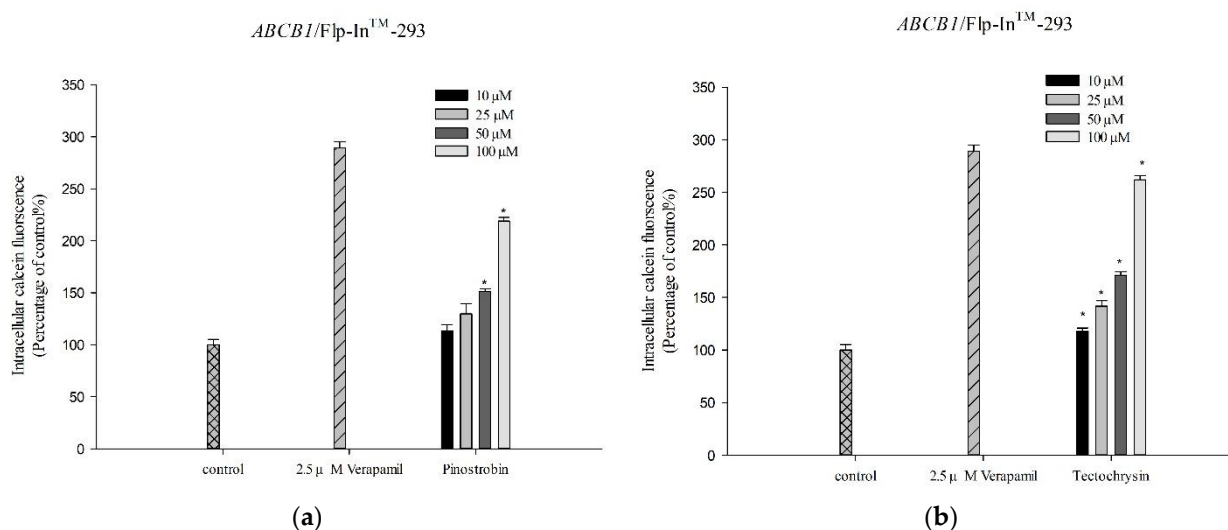


Figure 2. Inhibitory effects of pinostrobin (a) and tectochrysin (b) on human P-gp. Verapamil is a known P-gp inhibitor and was used as a positive control in our study. Data are presented as mean \pm standard error. * indicates comparison with the control; $p < 0.05$.

To investigate the enzyme kinetics associated with the effects of pinostrobin and tectochrysin on human P-gp, we performed rhodamine 123 and doxorubicin efflux assays. Rhodamine 123 and doxorubicin are well-known fluorescent substrates of P-gp. Their effluxes followed Michaelis–Menten kinetics; the kinetic parameters were analyzed. Although pinostrobin and tectochrysin decreased the maximal efflux rate (V_m) of rhodamine 123, the compounds did not affect the affinity (K_m) of P-gp (Tables 1 and 2; Figures 3 and 4). These findings suggested that pinostrobin and tectochrysin noncompetitively inhibited the efflux of rhodamine 123 through P-gp. Similar results were obtained for doxorubicin. Thus, pinostrobin and tectochrysin noncompetitively inhibit drug efflux through human P-gp.

Table 1. Kinetic parameters of P-gp-mediated effluxes of rhodamine 123 and doxorubicin in ABCB1/Flp-InTM-293 cells treated with pinostrobin.

	Nonlinear Kinetic Parameters	
	V_m (pmol/mg Protein/10 min)	K_m (μ M)
Nonlinear regression		
Rhodamine 123 only	16.27 \pm 0.43	12.86 \pm 0.78
+50 μ M Pinostrobin	13.77 \pm 0.29 *	12.22 \pm 0.50
+100 μ M Pinostrobin	11.45 \pm 0.15 *	12.42 \pm 0.24
	V_m (pmol/mg Protein/25 min)	K_m (μ M)
Nonlinear regression		
Doxorubicin only	1.80 \pm 0.06	0.06 \pm 0.004
+50 μ M Pinostrobin	1.63 \pm 0.01 *	0.06 \pm 0.002
+100 μ M Pinostrobin	1.32 \pm 0.01 *	0.06 \pm 0.002

V_m is the maximal efflux rate of rhodamine 123 or doxorubicin. K_m represents the Michaelis–Menten constant. * indicates comparison with nontreatment (rhodamine 123 or doxorubicin only); $p < 0.05$.

Table 2. Kinetic parameters of human P-gp-mediated effluxes of rhodamine 123 and doxorubicin in ABCB1/Flp-InTM-293 cells treated with tectochrysin.

	Nonlinear Kinetic Parameters	
	V_m (pmol/mg Protein/10 min)	K_m (μM)
Nonlinear regression		
Rhodamine 123 only	14.8 ± 0.57	17.33 ± 0.70
+50 μM Tectochrysin	$10.64 \pm 0.15^*$	16.45 ± 0.47
+100 μM Tectochrysin	$7.72 \pm 0.11^*$	16.04 ± 0.53
	V_m (pmol/mg Protein/25 min)	K_m (μM)
Nonlinear regression		
Doxorubicin only	3.74 ± 0.04	0.14 ± 0.002
+50 μM Tectochrysin	$3.12 \pm 0.04^*$	0.14 ± 0.004
+100 μM Tectochrysin	$2.85 \pm 0.004^*$	0.14 ± 0.001

V_m is the maximal efflux rate of rhodamine 123 or doxorubicin. K_m represents the Michaelis–Menten constant. * indicates comparison with nontreatment (rhodamine 123 or doxorubicin only); $p < 0.05$.

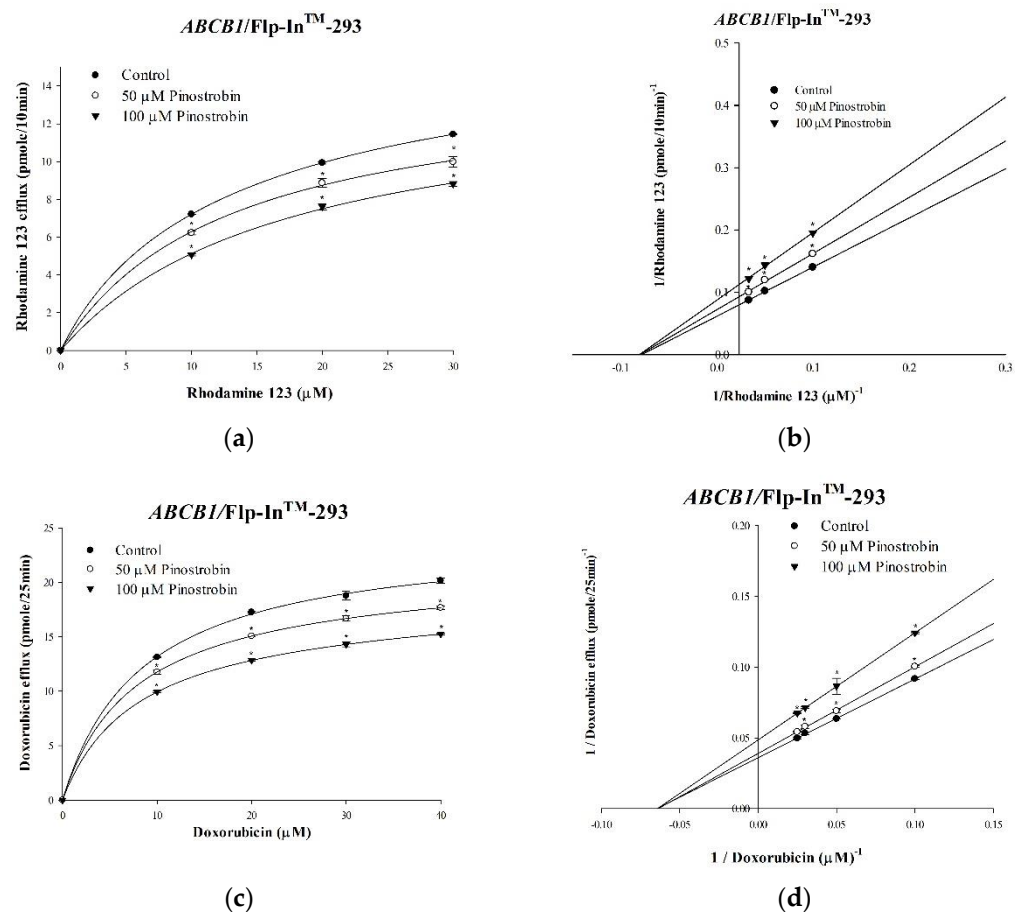


Figure 3. Pinostrobin–mediated inhibition: kinetic mechanisms underlying the P-gp-mediated effluxes of rhodamine 123 and doxorubicin. The saturation curve graphs indicate that the concentration-dependent effects of pinostrobin on the effluxes of rhodamine 123 (a) and doxorubicin (c) followed Michaelis–Menten kinetics. The Lineweaver–Burk plots present kinetics of the effluxes of rhodamine 123 (b) and doxorubicin (d). Data are presented as mean \pm standard. * indicates comparison with the untreated control; $p < 0.05$.

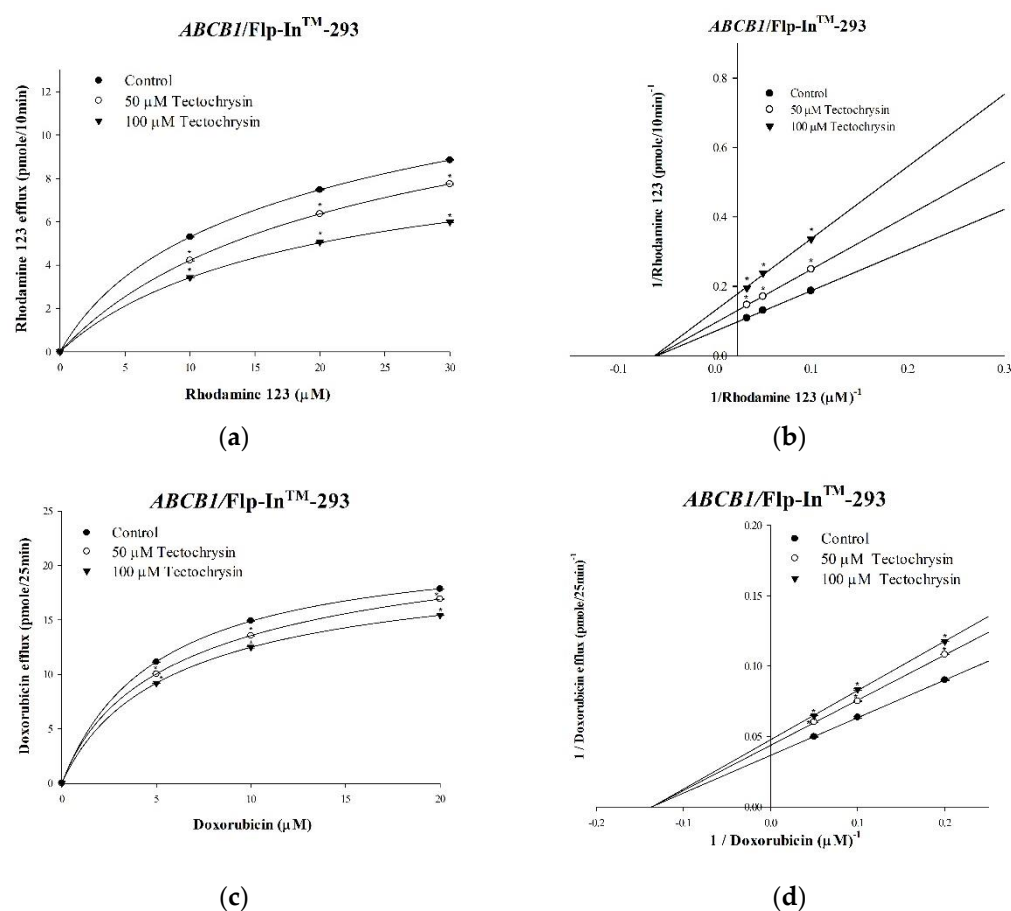


Figure 4. Tectochrysin—mediated inhibition: kinetic mechanisms underlying the P-gp-mediated effluxes of rhodamine 123 and doxorubicin. The saturation curve graphs indicate that the concentration-dependent effects of tectochrysin on the effluxes of rhodamine 123 (a) and doxorubicin efflux (c) followed Michaelis–Menten kinetics. The Lineweaver–Burk plots present the kinetics of the effluxes of rhodamine 123 (b) and doxorubicin (d). Data are presented as mean \pm standard deviation. * indicates comparison with the untreated control; $p < 0.05$.

2.2. Effects of Pinostrobin and Tectochrysin on the Conformation, ATPase Activity, and Expression of P-Gp

Whether pinostrobin and tectochrysin are the substrates of human P-gp was evaluated through the MDR1 shift assay. Vinblastine, a substrate of human P-gp, increased the fluorescence of cells treated with MDR1/ABCB1 antibody (UIC2); thus, it was regarded as a positive control. As shown in Figure 5, although pinostrobin and tectochrysin affected the fluorescence of cells treated with UIC2, they markedly reduced, and not increased, the fluorescence compared with the control. Hence, pinostrobin or tectochrysin is not a substrate of human P-gp.

To investigate whether pinostrobin and tectochrysin affected the activity of human P-gp ATPase, we performed the Pgp-GloTM assay. As shown in Figure 6, both pinostrobin and tectochrysin inhibited the basal ATPase activity of P-gp. Furthermore, pinostrobin and high concentration of tectochrysin inhibited the verapamil-stimulated ATPase activity of P-gp (Figure 6).

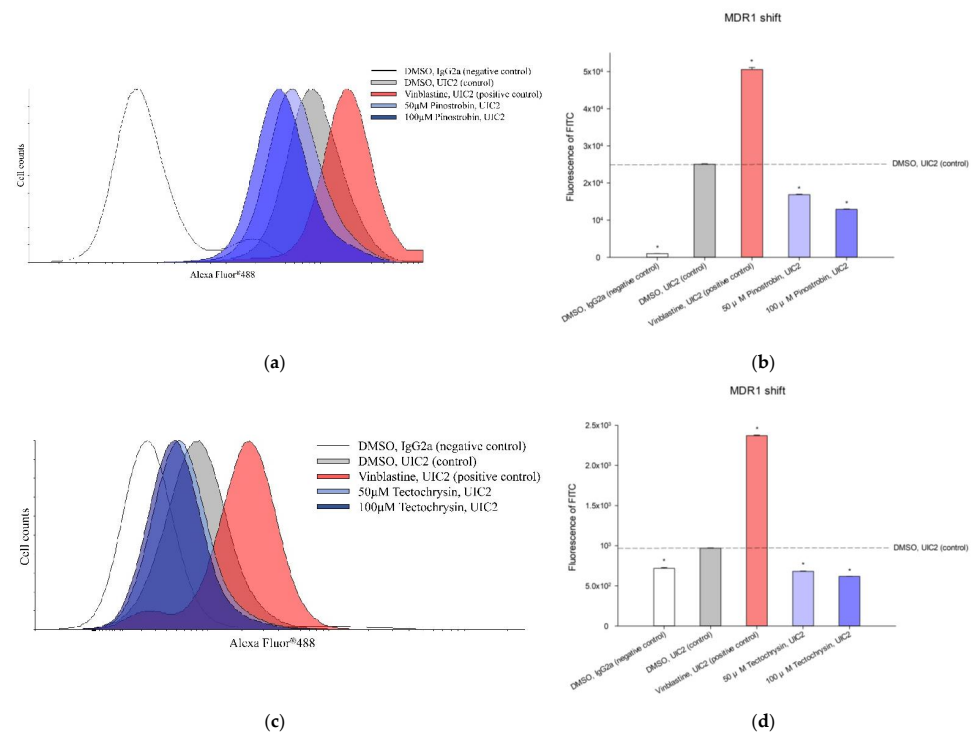


Figure 5. Effects of pinostrobin (a,b) and tectochrysin (c,d) on the conformation of human P-gp. The peak graphs (a,c) display the peak positions of fluorescence for different treatments, and the bar charts (b,d) present statistical data. The MDR1/ABCB1(UIC2) antibody is sensitive to the open conformation of P-gp. IgG2a antibody served as the negative control, whereas vinblastine served as the positive control. Data are presented as mean ± standard error values. * indicates comparison with the dimethyl sulfoxide control; $p < 0.05$.

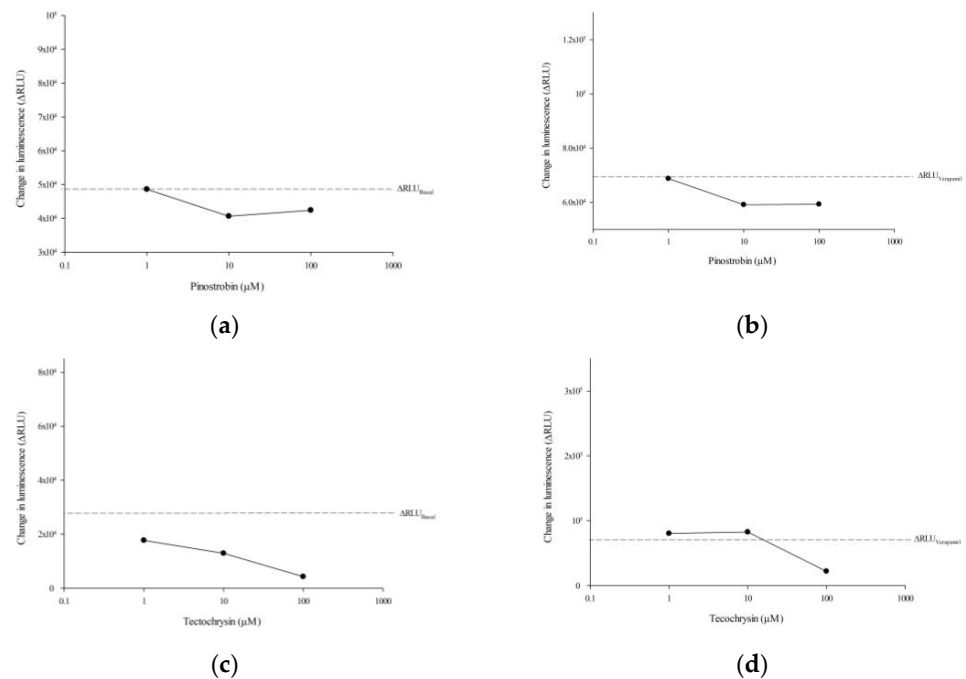


Figure 6. Effects of pinostrobin (a,b) and tectochrysin (c,d) on the ATPase activity of human P-gp. The left panels indicate the effects of pinostrobin (a) and tectochrysin (c) on ATPase activity, whereas the right panels indicate the effects of pinostrobin (b) and tectochrysin (d) on verapamil-induced ATPase activity. ΔRLU represents the changes in luminescence. Data are presented as mean ± standard error.

The effects of pinostrobin and tectochrysin on the expression levels of P-gp were investigated through Western blotting. After 48 h of incubation with pinostrobin or tectochrysin, the expression level of human P-gp in human oral squamous carcinoma (KB) cells was inapparent (Figure 7). The expression levels of P-gp were slightly affected in the resistant KBvin cell line; however, no significant differences were observed between the control and treatment groups (Figure 7). Hence, pinostrobin and tectochrysin may not affect the expression levels of P-gp.

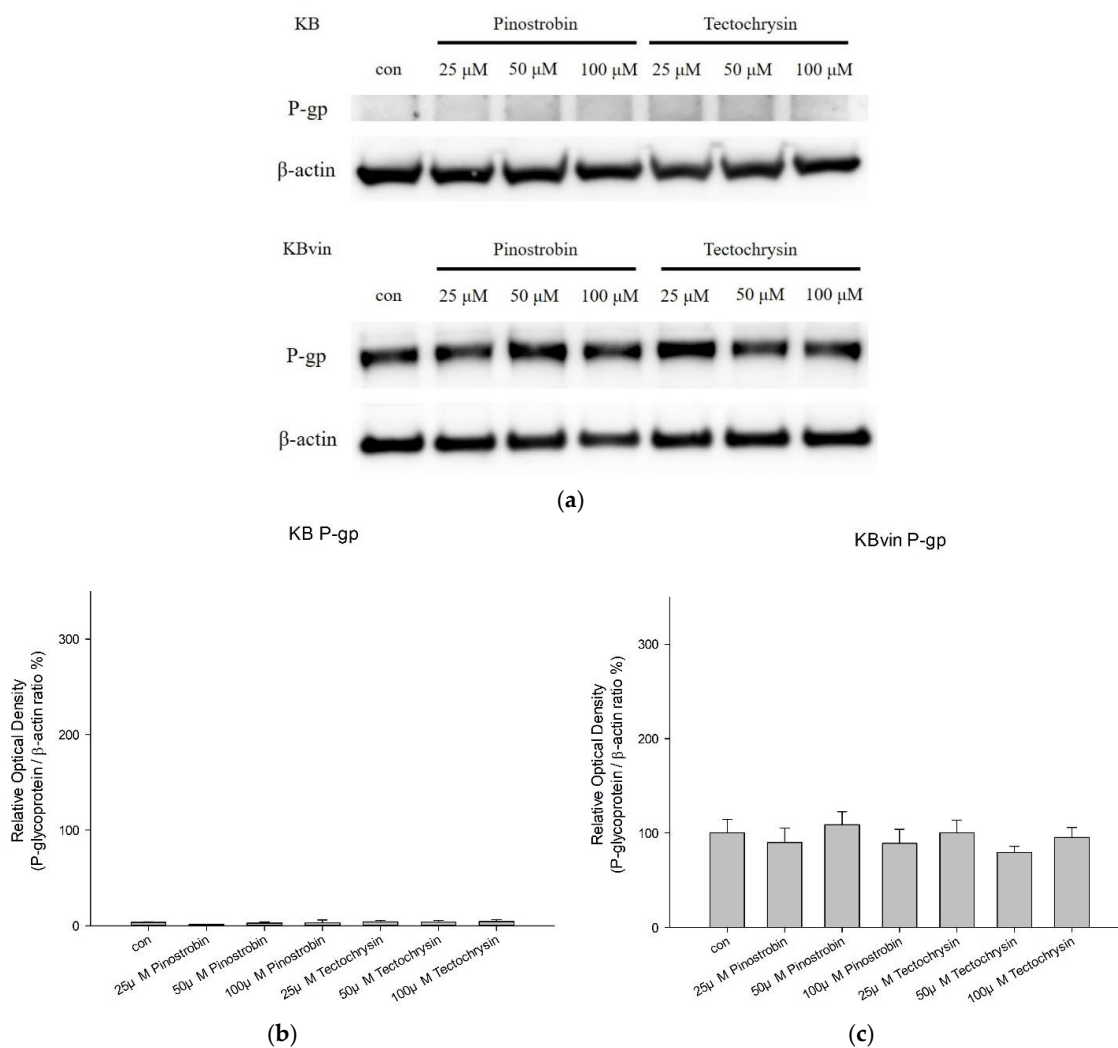


Figure 7. Effects of pinostrobin and tectochrysin on the expression of P-gp. (a) Results of the comparison between the control and test compounds (pinostrobin and tectochrysin) in terms of Western blotting data obtained using the isolates of pinostrobin or tectochrysin -treated (48 h) KB and KBvin cells. Bar charts presenting the changes in relative optical density (compared with the findings in the KBvin control group) in KB (b) and KBvin (c) cells. Data are presented as mean \pm standard error.

2.3. Potential of Pinostrobin and Tectochrysin for MDR Reversal and Underlying Mechanisms

As shown in Table 3, the IC_{50} values of pinostrobin and tectochrysin in a total of four cell lines were considerably higher than 100 μ M; hence, in the subsequent experiments, we used the concentration of < 100 μ M. The IC_{50} values of paclitaxel, vincristine, and docetaxel against KBvin and *ABCB1*/Flp-InTM-293 cells were significantly higher than those against human cervical adenocarcinoma (HeLa S3) and Flp-InTM-293 cells, respectively. Thus, the KBvin and *ABCB1*/Flp-InTM-293 cell lines were highly resistant to chemotherapeutic

drugs. When the concentrations of the test compounds were reduced in the combination treatments, the corresponding IC₅₀ values of the resistant cell lines reduced synergistically, and the reversal fold values increased substantially (Tables 4 and 5). Drug–drug interactions between pinostrobin or tectochrysin and chemotherapeutic drugs were determined through combination index (CI) analysis. As shown in Table 6, the CI values of pinostrobin and three chemotherapeutic drugs ranged from 0.092 to 0.523, indicating the synergist effects of the combination treatments. The CI values of tectochrysin and the three chemotherapeutic drugs were similar (0.023–0.839; Table 7). Therefore, pinostrobin and tectochrysin may exert synergistic effects on MDR reversal.

Table 3. IC₅₀ values (72 h) of pinostrobin and tectochrysin in four cell lines.

Cell Lines	IC ₅₀ (μM) ± SE	
	Pinostrobin	Tectochrysin
Flp-In TM -293	666.64 ± 7.01	281.58 ± 1.84
ABCBI/Flp-In TM -293	510.53 ± 4.85	242.17 ± 2.67
HeLa S3	530.05 ± 12.37	207.37 ± 2.88
KBvin	623.59 ± 68.65	229.87 ± 2.05

SE, standard error.

Table 4. IC₅₀ values (72 h) of the combination of pinostrobin or tectochrysin with three different chemotherapeutic drugs in HeLa S3 and KBvin cells.

Treatment	HeLa S3 (Drug Sensitive)		KBvin (Resistant)	
	IC ₅₀ (nM) ± SE	RF	IC ₅₀ (nM) ± SE	RF
Vincristine	6.30 ± 0.07		2860.66 ± 24.65	
+50 μM Pinostrobin	2.78 ± 0.03 *	2.27	332.24 ± 5.60 *	8.61
+100 μM Pinostrobin	0.95 ± 0.01 *	6.63	252.03 ± 4.42 *	11.35
+50 μM Tectochrysin	4.01 ± 0.03 *	1.57	382.19 ± 17.63 *	7.48
+100 μM Tectochrysin	2.38 ± 0.07 *	2.65	149.66 ± 20.86 *	19.11
Paclitaxel	10.36 ± 0.30		1178.73 ± 28.45	
+50 μM Pinostrobin	7.11 ± 0.04 *	1.46	217.94 ± 7.68 *	5.41
+100 μM Pinostrobin	5.90 ± 0.10 *	1.76	73.84 ± 1.16 *	15.96
+50 μM Tectochrysin	8.74 ± 0.24 *	1.19	202.09 ± 15.78 *	5.83
+100 μM Tectochrysin	5.34 ± 0.09	1.94	60.23 ± 0.13 *	19.57
Docetaxel	5.29 ± 0.07		267.33 ± 13.27	
+50 μM Pinostrobin	2.17 ± 0.10 *	2.44	18.90 ± 0.63 *	14.14
+100 μM Pinostrobin	0.64 ± 0.02 *	8.27	113.97 ± 0.69 *	19.13
+50 μM Tectochrysin	3.29 ± 0.14	1.61	8.85 ± 0.41 *	30.20
+100 μM Tectochrysin	0.61 ± 0.02 *	8.64	3.25 ± 0.13 *	82.26

RF, reversal fold; SE, standard error. RF = IC₅₀ values of chemotherapeutic drugs divided by those of the combination of chemotherapeutic drugs with either pinostrobin or tectochrysin. * indicates comparison with noncombination (chemotherapeutic drugs only); *p* < 0.05.

The relative division index values of the KB and KBvin cell lines increased in a time-dependent manner. With time, the fluorescence peak shifted toward the left because the fluorescence due to carboxyfluorescein succinimidyl ester (CFSE) decreased with cell division (Figures 8a and S1). In KB cells, although tectochrysin increased the relative division index value after 48 h, pinostrobin and tectochrysin reduced the index value after 72 h. By contrast, the test compounds substantially decreased the index values both at 48 h and 72 h in KBvin cells (Figure 8b,c). As shown in the overlapped peak graph, compared with the findings obtained through the control treatment, the peaks of cells treated with the test compounds, particularly pinostrobin, shifted toward the right. Therefore, pinostrobin and tectochrysin may inhibit the proliferation of cells. The effects of pinostrobin on cell proliferation were stronger than those of tectochrysin (Figure S1).

Table 5. IC₅₀ values (72 h) of the combination of pinostrobin or tectochrysin with three different chemotherapeutic drugs in Flp-InTM-293 and ABCB1 overexpressing Flp-InTM-293 cells.

Treatment	Flp-In TM -293 Cell (Parental)		ABCB1/Flp-In TM -293 Cell (Resistant)	
	IC ₅₀ (nM) ± SE	RF	IC ₅₀ (nM) ± SE	RF
Vincristine	7.62 ± 0.11		855.97 ± 11.91	
+50 µM Pinostrobin	1.09 ± 0.05 *	6.99	98.93 ± 1.40 *	8.65
+100 µM Pinostrobin	0.78 ± 0.02 *	9.79	60.21 ± 0.98 *	14.22
+50 µM Tectochrysin	3.95 ± 0.03 *	1.93	91.71 ± 1.70 *	9.33
+100 µM Tectochrysin	3.01 ± 0.12 *	2.53	62.94 ± 0.67 *	13.60
Paclitaxel	12.98 ± 1.72		850.14 ± 19.34	
+50 µM Pinostrobin	6.87 ± 0.12	1.89	231.67 ± 10.05 *	3.67
+100 µM Pinostrobin	5.69 ± 0.07	2.28	41.70 ± 1.76 *	20.39
+50 µM Tectochrysin	7.86 ± 0.14	1.65	90.79 ± 1.91 *	9.36
+100 µM Tectochrysin	7.32 ± 0.17	1.77	68.59 ± 1.57 *	12.39
Docetaxel	6.92 ± 0.12		140.86 ± 11.60	
+50 µM Pinostrobin	5.15 ± 0.17 *	1.34	22.47 ± 1.00 *	6.27
+100 µM Pinostrobin	1.40 ± 0.14 *	4.95	3.96 ± 0.24 *	35.61
+50 µM Tectochrysin	5.61 ± 0.34 *	1.23	6.83 ± 0.11 *	20.64
+100 µM Tectochrysin	3.39 ± 0.30 *	2.04	5.35 ± 0.08 *	26.32

RF, reversal fold; SE, standard error. RF = IC₅₀ values of chemotherapeutic drugs divided by those of the combination of chemotherapeutic drugs with either pinostrobin or tectochrysin. * indicates comparison with noncombination (chemotherapeutic drugs only); $p < 0.05$.

Table 6. Combination index values of the combinations of pinostrobin with vincristine, paclitaxel, and docetaxel in MDR KBvin cells.

Pinostrobin	[Vincristine]	Fraction Affected (Fa)	Combination Index (CI)	Drug Interaction Description
50 µM	1000 nM	0.098	0.132	Strong synergism
	100 nM	0.630	0.228	Strong synergism
100 µM	1000 nM	0.049	0.092	Very Strong Synergism
	100 nM	0.599	0.355	Synergism
Pinostrobin	[Paclitaxel]	Fraction affected (Fa)	Combination index (CI)	Drug interaction description
50 µM	100 nM	0.574	0.217	Strong synergism
	10 nM	0.740	0.336	Synergism
100 µM	100 nM	0.432	0.181	Strong synergism
	10 nM	0.51	0.405	Synergism
Pinostrobin	[Docetaxel]	Fraction affected (Fa)	Combination index (CI)	Drug interaction description
50 µM	100 nM	0.026	0.093	Very Strong Synergism
	10 nM	0.540	0.197	Strong synergism
100 µM	100 nM	0.300	0.523	Synergism
	10 nM	0.505	0.275	Strong synergism

CI < 1, synergism; CI = 1, additive effect; and CI > 1, antagonism.

Table 7. Combination index values of the combinations of tectochrysin with vincristine, paclitaxel, and docetaxel in MDR KBvin cells.

Tectochrysin	[Vincristine]	Fraction Affected (Fa)	Combination Index (CI)	Drug Interaction Description
50 μM	1000 nM	0.126	0.215	Strong synergism
	100 nM	0.684	0.389	Synergism
100 μM	1000 nM	0.046	0.160	Strong synergism
	100 nM	0.578	0.560	Synergism
Tectochrysin	[Paclitaxel]	Fraction affected (Fa)	Combination index (CI)	Drug interaction description
50 μM	100 nM	0.594	0.357	Synergism
	10 nM	0.895	0.839	Moderate synergism
100 μM	100 nM	0.292	0.277	Strong synergism
	10 nM	0.763	0.859	Strong synergism
Tectochrysin	[Docetaxel]	Fraction affected (Fa)	Combination index (CI)	Drug interaction description
50 μM	100 nM	0.008	0.061	Very Strong Synergism
	10 nM	0.483	0.277	Strong synergism
100 μM	100 nM	0.001	0.023	Very Strong Synergism
	10 nM	0.125	0.169	Strong synergism

CI < 1, synergism; CI = 1, additive effect; and CI > 1, antagonism.

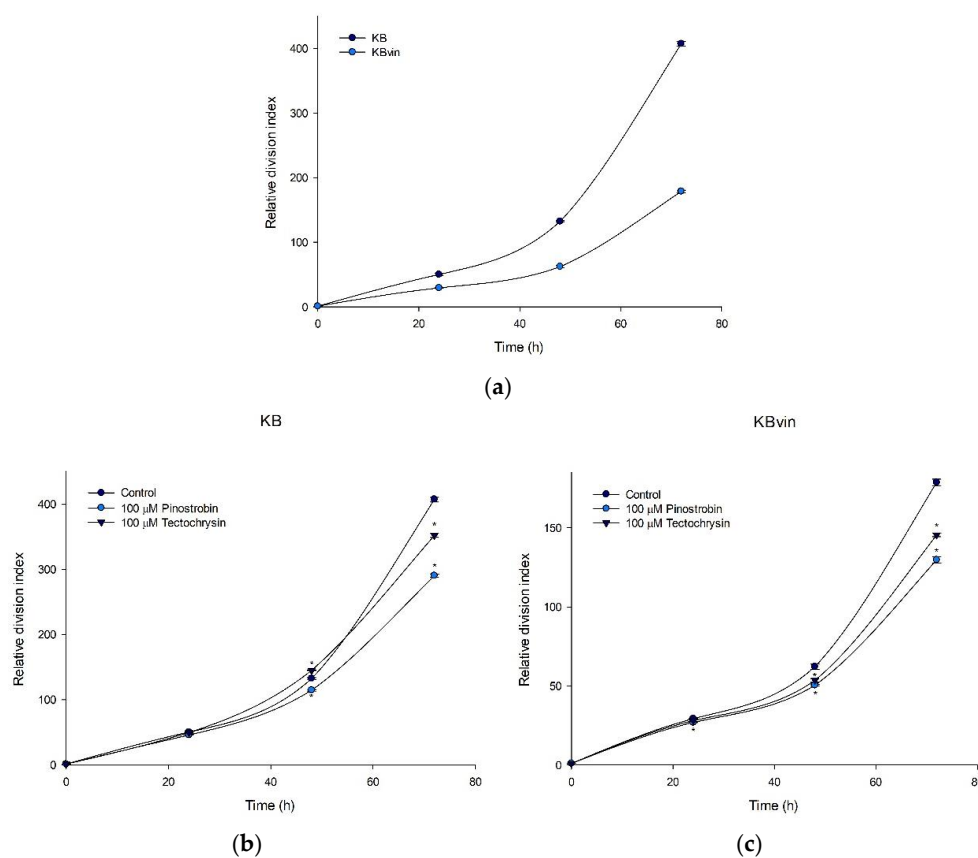


Figure 8. Effects of pinostrobin and tectochrysin on the proliferation of cells. The relative division index was inverse-normalized using the 0-h fluorescence level. (a) Basal division index of the KB and KBvin cell lines. (b,c) Curved graphs presenting the index of the control, pinostrobin, and tectochrysin treatments in the KB and KBvin cell lines, respectively. Data are presented as mean ± standard error. * indicates comparison with the control; $p < 0.05$.

As shown in Figures 9 and 10, the treatment of cells with only paclitaxel or vincristine led to normal cell cycle distribution; similar results were obtained for pinostrobin and tectochrysin treatments. The combination of pinostrobin and chemotherapeutic drugs increased the proportion of apoptotic cells and reduced the proportion of cells in the G1 phase of the cell cycle. By contrast, the combination of tectochrysin and chemotherapeutic drugs increased the proportions of HeLa S3 cells in the S phase of the cell cycle and those of KBvin cells in the sub-G1 phase of the cell cycle.

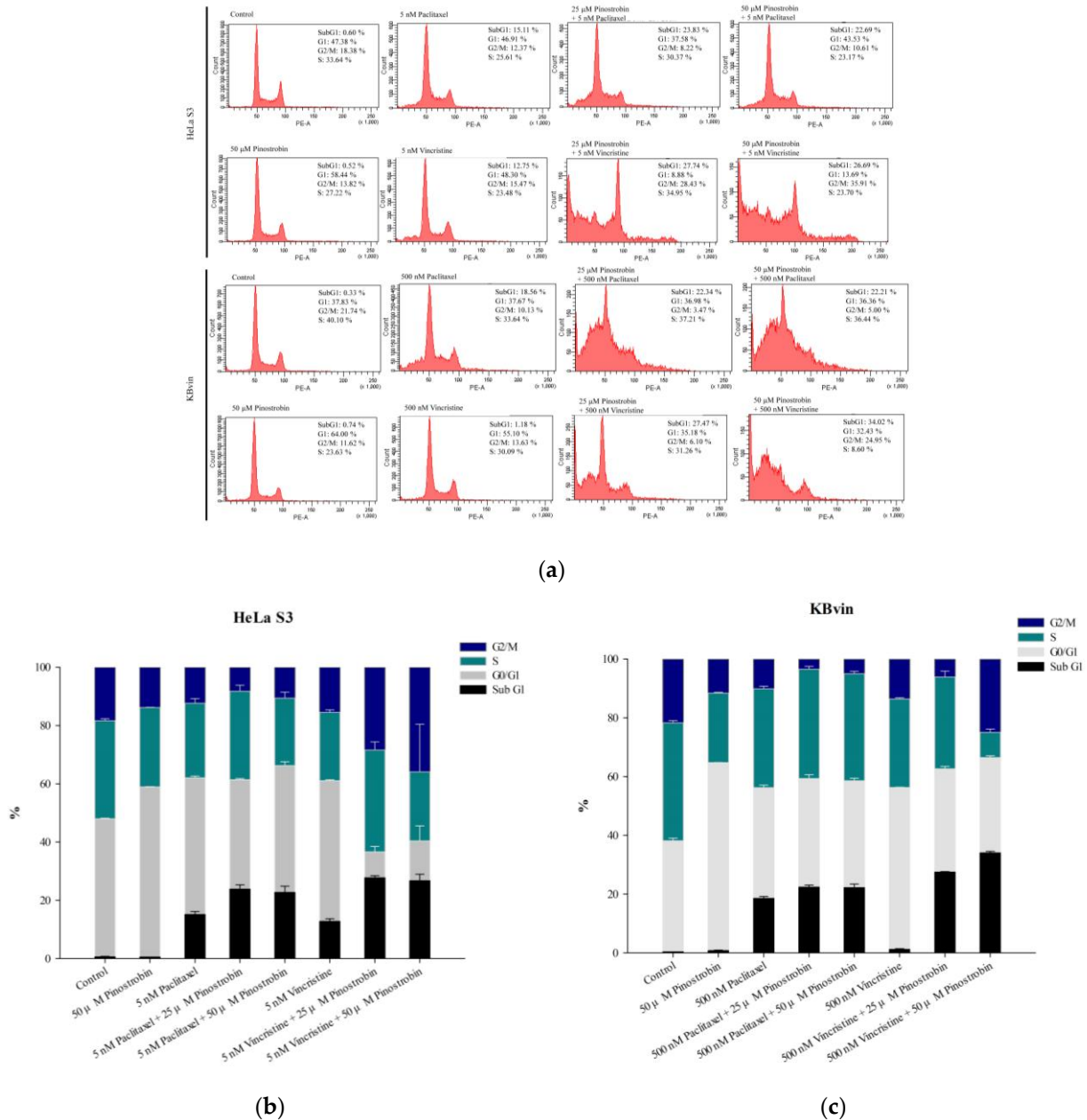
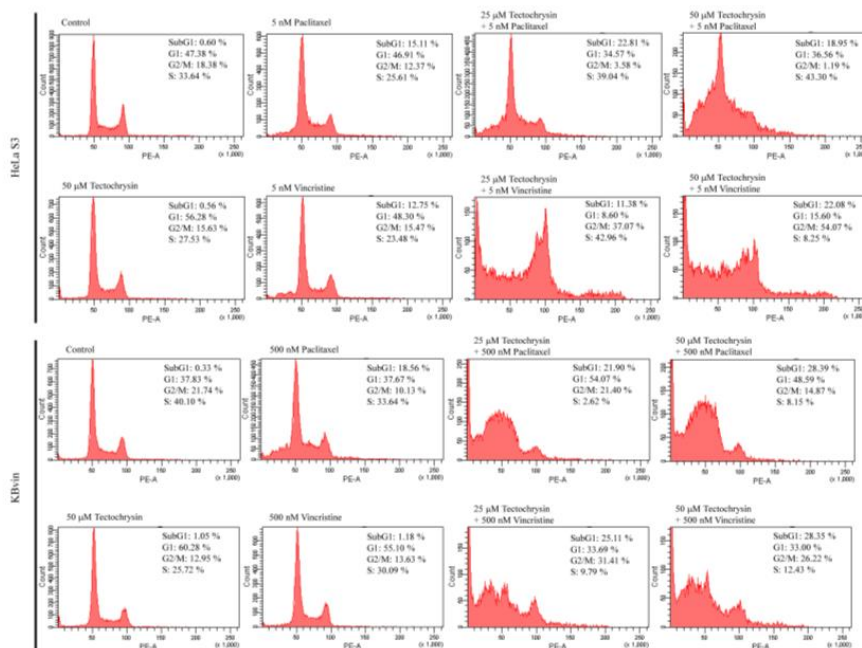
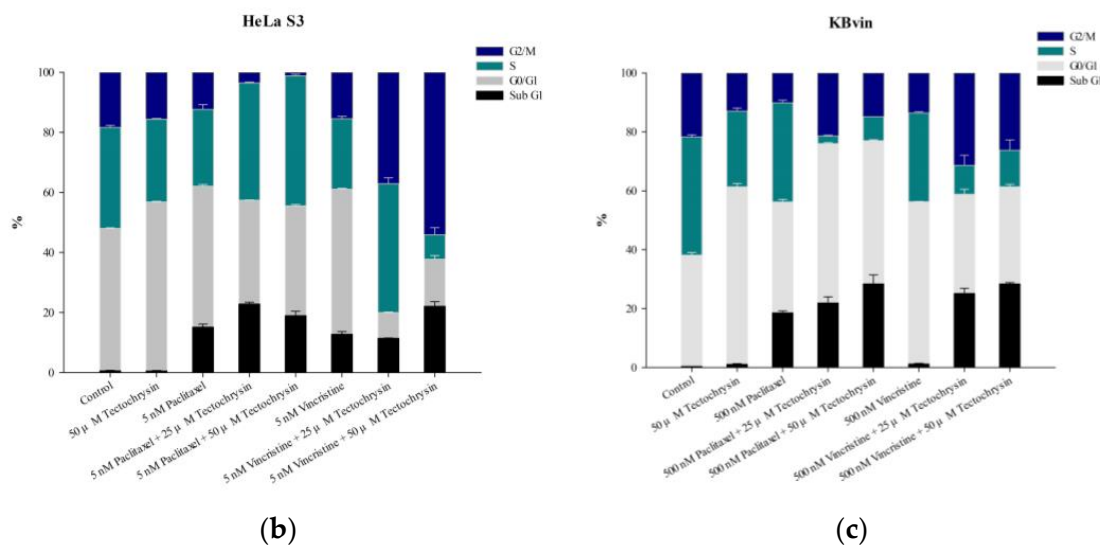


Figure 9. Effects of pinostrobin on the cell cycle in the HeLa S3 and KBvin cell lines. (a) Cell cycle was assessed through flow cytometry performed after the treatment of the aforementioned cells with pinostrobin for 48 h. The bar charts depict the proportions of HeLa S3 (b) and KBvin (c) cells in various phases of the cell cycle. Data are presented as mean ± standard error.



(a)



(b)

(c)

Figure 10. Effects of tectochrysin on the cell cycle in the HeLa S3 and KBvin cell lines. (a) Cell cycle was assessed through flow cytometry performed after the treatment of HeLa S3 and KBvin cells with tectochrysin for 48 h. The bar charts depict the proportions of HeLa S3 (b) and KBvin (c) cells in various phases of the cell cycle. Data are presented as mean ± standard error.

The pattern of cell death was assessed using the HeLa S3 and KBvin cancer cell lines. As shown in Figures 11 and 12, the combination treatments induced early apoptosis and late apoptosis in the two cell lines. In MDR KBvin cells, the proportion of live cells decreased, and that of late apoptotic cells markedly increased. Hence, pinostrobin and tectochrysin may enhance the cytotoxic effects of chemotherapeutic drugs.

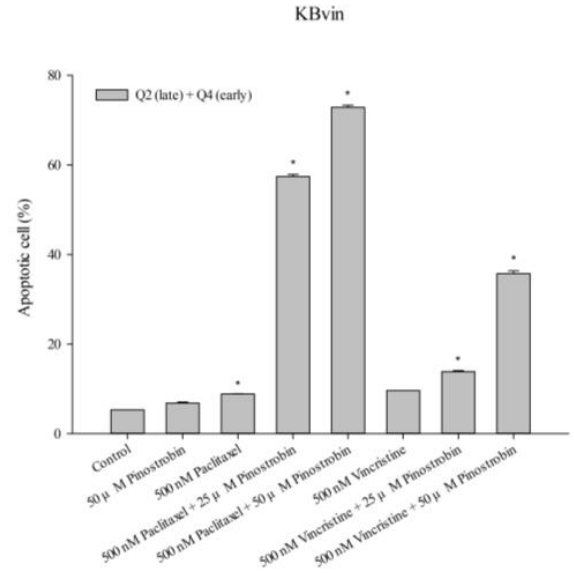
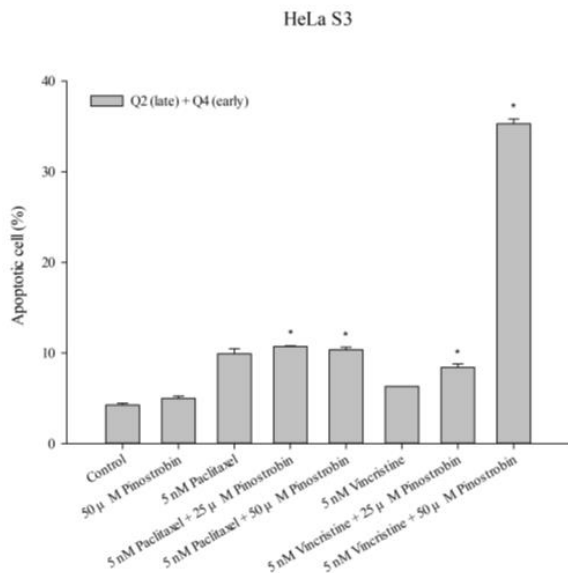
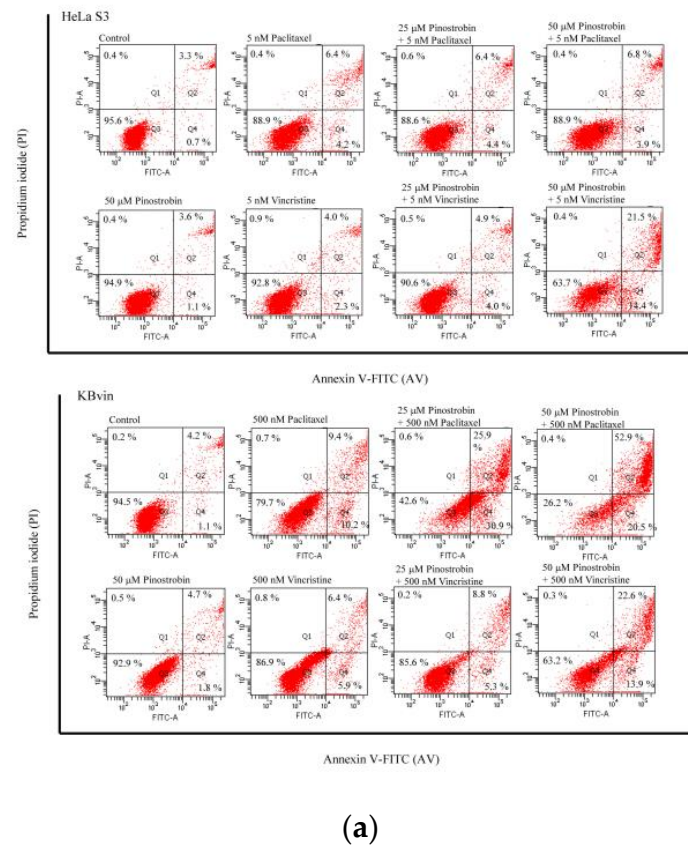


Figure 11. Death pattern of HeLa S3 and KBvin cells. (a) Apoptotic cells were assessed through flow cytometry performed after the treatment of HeLa S3 and KBvin cells with pinstrobin for 48 h. The bar charts depict the proportions of apoptotic cells in the HeLa S3 (b) and KBvin (c) cell lines. Data are presented as mean \pm standard. * indicates comparison with the control; $p < 0.05$.

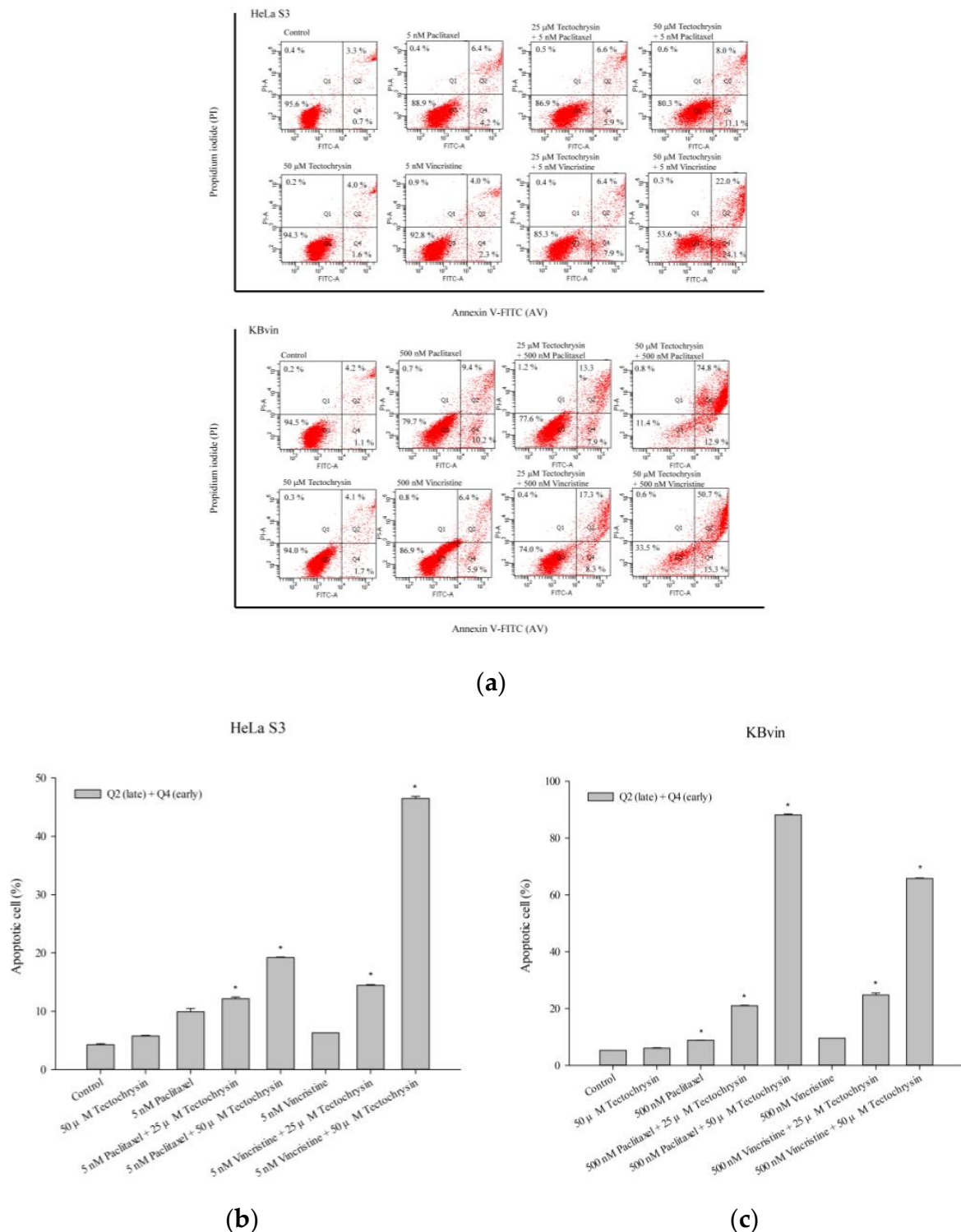


Figure 12. Death pattern of HeLa S3 and KBvin cells. (a) Apoptotic cells were assessed through flow cytometry performed after the treatment of the HeLa S3 and KBvin cells with tectochrysin for 48 h. The bar charts depict the proportions of apoptotic cells in the HeLa S3 (b) and KBvin (c) cell lines. Data are presented as mean \pm standard deviation. * indicates comparison with the control; $p < 0.05$.

2.4. Molecular Docking of Pinostrobin and Tectochrysin on P-gp

The best docking interactions between the test compounds and human P-gp were simulated using AutoDock 4.2.6. Table 8 and Figure 13 present the binding energy levels

and amino acids involved in the docking interactions and hydrogen bonding. Pinostrobin, tectochrysin, and verapamil did not form hydrogen bonds with the amino acids in P-gp. For pinostrobin and tectochrysin, similar amino acids were involved in the interactions. Moreover, the value of the lowest binding energy was higher for verapamil, a standard inhibitor of P-gp, than for the test compounds. Therefore, the affinities of pinostrobin and tectochrysin toward human P-gp may be better than that of verapamil.

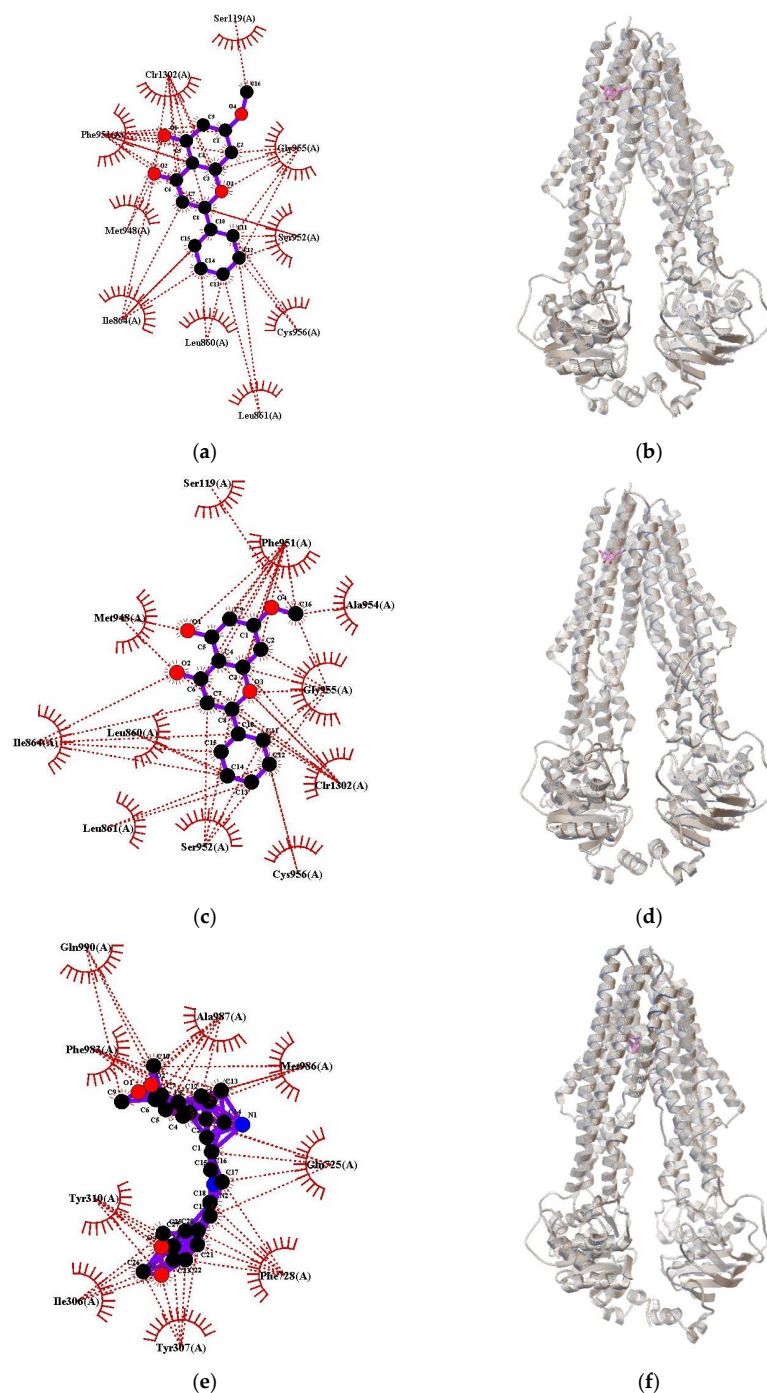


Figure 13. Two-dimensional and three-dimensional models of molecular docking of pinostrobin, tectochrysin, and verapamil on P-gp. Two-dimensional models showing the interactions among the ligands pinostrobin (a), tectochrysin (c), and verapamil (e). Three-dimensional models showing the adducts of pinostrobin (b), tectochrysin (d), and verapamil (f) with P-gp. Verapamil is a P-gp inhibitor.

Table 8. Results of the molecular docking of pinostrobin, tectochrysin, and verapamil.

	Lowest Binding Energy (kcal/mol)	Mean Binding Energy (kcal/mol)	predKi	Td	CR	Number of Runs in 1st Cluster	Amino Acids Involved in Interactions	Amino Acids Involved in H-Bonds
Pinostrobin	−8.26	−8.07	882.38 nM	2	11	10	Clr1302, Cys956, Gly955, Ile864, Leu860, Leu861, Met948, Phe951, Ser119, Ser952	None
Tectochrysin	−8.17	−7.98	1.03 μM	2	7	9	Ala954, Clr1302, Cys956, Gly955, Ile864, Leu860, Leu861, Met948, Phe951, Ser119, Ser952	None
Verapamil	−5.57	−3.21	82.19 μM	17	29	4	Ala987, Gln725, Gln990, Ile306, Met986, Phe728, Phe983, Tyr307, Tyr310	None

The lowest and mean binding energy levels predicted inhibition constant (predKi) values, torsdof parameter (Td) numbers, and cluster ranks (CRs) of the test compounds and verapamil. The amino acids involved in the docking interactions are also presented.

3. Discussion

In the present study, pinostrobin and tectochrysin exerted inhibitory effects on P-gp. The results of the P-gp ATPase activity assay and kinetic analysis revealed that pinostrobin and tectochrysin inhibited drug efflux through P-gp by hindering its ATPase activity and noncompetitively inhibiting the transport of drugs, namely rhodamine 123 and doxorubicin. In addition, pinostrobin and tectochrysin restored the sensitivity of MDR cancer cells to chemotherapeutic drugs, such as paclitaxel, vincristine, docetaxel, thus exhibiting strong MDR reversal activity. These findings suggest that pinostrobin and tectochrysin are promising candidates for treating cancer synergistically.

In chemotherapy, the development of MDR remains the predominant obstacle. Enhanced drug efflux by ABC transporters is a key mechanism underlying MDR. The induction of P-gp expression in cancer cells is associated with poor clinical outcomes and reduced chemotherapeutic responses in various cancer types. Thus, P-gp has been regarded as a potential target for overcoming MDR in cancer [17]. Although early inhibitors, such as valspodar, were shown to inhibit cytochrome P450 and lead to chemotherapy dose reductions, third generation inhibitors were nontoxic and effective. However, the clinical benefits of P-gp inhibitors are yet to be confirmed owing to the absence of P-gp in patients' tumors. These clinical trials did not examine whether these tumors expressed P-gp or not. Tariquidar could reverse the doxorubicin-resistance in mouse model [17–20].

Owing to their low cytotoxicity and high oral bioavailability, natural compounds or plant extracts, such as flavonoids, alkaloids, terpenoids, and coumarins, can serve as potent P-gp inhibitors [17,21]. Genistein and naringenin have been demonstrated to increase the accumulation of topotecan in K562/BCRP cells by modulating ABC transporters [22]. Curcumin has been reported to reduce the expression level of P-gp for enhancing the cytotoxicity of paclitaxel and adriamycin in SKOV3(TR) and K562/A02 cells [23,24]. Furthermore, glaucine has been shown to not only inhibit ABC transporters but also reduce the expression levels of MDR1 and MRP1 [25]. In addition to affecting the activity and expression of transporters, phytochemicals, such as glaucine, nobiletin, and antofine, can resensitize cancer cells to chemotherapeutic drugs through synergism [3].

Pinostrobin induces cancer cell apoptosis through the reactive oxygen species (ROS)-mediated extrinsic and intrinsic signaling pathways and ROS-mediated mitochondrial damage [17]. By contrast, tectochrysin has been demonstrated to induce apoptosis in prostate cancer cells by affecting the TNF- α -related apoptosis-inducing ligand and phosphatidylinositol 3-kinase/protein kinase B signaling pathways, suppressing NF- κ B activity, and increasing the expression levels of death receptors in colon cancer cells [8,18]. Tectochrysin has been identified to be a potent inhibitor of ABCG2 [11]. However, its inhibitory effects on P-gp remain unclear. In the present study, we demonstrated that pinostrobin and tectochrysin affected the proliferation of drug-resistant cancer cells; nonetheless, the combination of pinostrobin or tectochrysin with chemotherapeutic drugs exhibited substantial

cytotoxicity. Pinostrobin and tectochrysin enhanced the cytotoxicity of chemotherapeutic drugs by inhibiting the efflux of chemotherapeutic drugs and exerted synergistic effects on MDR cancer cells to resensitize them to chemotherapeutic drugs.

In terms of P-gp binding sites, the H-site preferentially interacts with Hoechst 33258, Hoechst 33342, colchicine, and quercetin, whereas the R-site preferentially binds daunorubicin, rhodamine 123, doxorubicin, and other anthracyclines. Furthermore, compounds that block substrate efflux may bind to the M-site on P-gp, which is a modulator site. The P-gp substrates rhodamine 123 and doxorubicin may recognize and bind to the R-site, whereas rhodamine 123 binds to the M-site [26]. In our kinetic analysis, pinostrobin and tectochrysin noncompetitively inhibited drug (rhodamine 123 and doxorubicin) efflux through P-gp. This finding implies that pinostrobin and tectochrysin bind to the H-site or other unknown binding sites on P-gp. Through docking analysis, we observed that the two test compounds had similar binding residues on P-gp, which differed from those of verapamil. The level of the lowest binding energy was higher for verapamil than for pinostrobin and tectochrysin. The torsdof parameter, which indicates free rotatable bonds, revealed that verapamil has several rotatable bonds. This explains the difficulty in predicting optimal docking of verapamil with P-gp [27].

In addition to drug-binding sites, P-gp has two ATP-binding sites. Compared with basal activity, ATPase activity was inhibited in the presence of pinostrobin and tectochrysin. Pinostrobin and a high concentration of tectochrysin inhibited the verapamil-stimulated ATPase activity of P-gp and the concentrations of pinostrobin and tectochrysin were found to be inversely correlated with ATPase activity. This finding suggests that the affinities of pinostrobin and tectochrysin for ATPase may be stronger than that of verapamil. Regarding the conformation of P-gp, vinblastine—a substrate of P-gp—markedly increased fluorescence and altered P-gp conformation. By contrast, pinostrobin and tectochrysin reduced fluorescence and slightly modified the P-gp conformation. The effects of the test compounds were weaker than that of vinblastine. Therefore, pinostrobin and tectochrysin may not be the substrates of P-gp. This is advantageous because had the compounds been P-gp substrates, higher concentrations of the compounds would have been required for the effective inhibition of P-gp-mediated drug efflux.

Our study has several strengths. For example, we used a cell line that stably expressed human P-gp (*ABCB1*/Flp-InTM-293) to elucidate the mechanisms underlying the effects of test compounds; this avoided interference from other transporters. Furthermore, to mimic the tumor environment in clinical conditions, we used an MDR cancer cell line. Compared to previous three generations of inhibitors, pinostrobin and tectochrysin, as natural compounds, have lower cytotoxicity and better oral bioavailability. With low cytotoxic profiles, these natural products may serve as daily supplements and may provide better disease control via increasing efficacy of chemotherapeutic agents. In addition, they may consider as leads for future drug designs. Previously, Mohana et al. [16] have demonstrated that the results of pinostrobin docking to P-gp and QSAR prediction. They did not mention any results about tectochrysin and conduct any in vitro experiments related to these compounds. In addition, Ahmed-Belkacem, A et al. [15] have evidenced that tectochrysin is a potent inhibitor of ABCG2-mediated drug efflux but have not investigated the effect on P-gp activity in depth. To the best of our knowledge, the present study is the first to investigate the inhibitory effects of pinostrobin and tectochrysin on P-gp and the underlying molecular mechanisms.

The major limitation of the present study is a lack of in vivo evidence. In a relevant study [12], the anticancer effect of tectochrysin was investigated in an animal model; however, more in vivo studies are needed to validate the efficacy of the test compounds for MDR reversal. The overexpression of P-gp might play a crucial role in clinical drug resistance in a few cases, not in most drug-resistant patients [18,28].

In the present study, we investigated the MDR reversal potential and P-gp inhibitory effects of pinostrobin and tectochrysin. Our findings revealed the detailed mechanisms underlying the inhibitory effects of the aforementioned compounds on ATP consumption

and human P-gp conformation. Pinostrobin and tectochrysin may be promising P-gp modulators. This study may serve as a reference for future studies aimed at developing treatment strategies for patients with MDR cancer.

4. Materials and Methods

4.1. Chemical Compounds and Reagents

Pinostrobin, tectochrysin, dimethyl sulfoxide (DMSO), acetic acid, ethanol (analytical and absolute grades), β -mercaptoethanol (β -ME), sulforhodamine B (SRB), Tris base, rhodamine 123, paclitaxel, vincristine, verapamil, calcein-AM, and trichloroacetic acid (TCA) were obtained from Sigma-Aldrich Co. (St Louis, MO, USA). Doxorubicin was purchased from United States Biological (Woburn, Massachusetts, USA). Zeocin was obtained from InvivoGen (San Diego, CA, USA). Roswell Park Memorial Institute (RPMI) 1640 medium and Dulbecco's Modified Eagle Medium (DMEM) were purchased from Thermo Fisher Scientific Inc. (Waltham, MA, USA). Phosphate buffered saline (PBS), hygromycin B, fetal bovine serum (FBS), and Trypsin-ethylenediamine tetra-acetic acid were obtained from Invitrogen (Carlsbad, CA, USA).

4.2. Cell Culture

Drug-sensitive HeLa S3 and KB cancer cell lines were from Bioresource Collection and Research Center (Hsinchu, Taiwan). The KBvin cell line was a generous gift from Dr. Kuo-Hsiung Lee (University of North Carolina, Chapel Hill, NC, USA). The parental cells Flp-InTM-293 were incubated with 100 μ g/mL zeocin. ABCB1-expressing cells (ABCB1/Flp-InTM-293) with the stable expression of human P-gp were cultured with 100 μ g/mL hygromycin B. The Flp-InTM-293 and ABCB1/Flp-InTM-293 cell lines were established as described previously [29]. A total of five cell lines were incubated in DMEM or RPMI 1640 with 10% FBS and incubated at 37 °C under 5% CO₂.

4.3. Cell Viability Assay and CI Analysis

The cells were treated with different concentrations of chemotherapeutic drugs, pinostrobin, tectochrysin, or their combination (pinostrobin or tectochrysin + chemotherapeutic drug) for 72 h. Then, 50% TCA was used to fix the living cells for 30 min. Subsequently, 0.04% SRB was used to stain the fixed cells for 30 min. Tris base (10 mM) was used to dissolve the attached SRB. Absorbance was recorded at 515 nm using a BioTek Synergy HT Multi-Mode Microplate Reader (Agilent, Santa Clara, CA, USA). Using CompuSyn software, CI values were determined on the basis of the IC₅₀ values of the test compounds and chemotherapeutic drugs. CI values of <1, 1, and >1, respectively, indicate synergism, additive effect, and antagonism in drug combination [30].

4.4. Cell Proliferation Assay

The effects of pinostrobin and tectochrysin on cell proliferation were evaluated using the CFSE Cell Labeling Kit (ab113853; Abcam, Cambridge, UK). The cells were harvested and suspended in 2 mL PBS. CFSE stock solution (10 mM; 2 μ L) was added to the cell suspension and incubated for 10 min at 37 °C. Next, the stained cells were washed with medium to remove the excess dye and were seeded in 6-well plates, which were subjected to pinostrobin or tectochrysin treatment for 72 h. Subsequently, the cells were harvested and resuspended in PBS. Fluorescence-activated cell sorting (FACS) analysis (BD FACSCantoTM II System; fluorescein isothiocyanate [FITC] channel) was performed to measure fluorescence levels. Relative division index was calculated by dividing the geometric mean of 0-h CFSE fluorescence with the CFSE fluorescence of different time points [31].

4.5. Calcein-AM Uptake assay

A calcein-AM uptake assay was performed to assess the effects of pinostrobin and tectochrysin on the efflux function of human P-gp. The density of the cells in 96-well plates was 1×10^5 cells/well. After incubation for 24 h, the cells were washed and pretreated

with pinostrobin, tectochrysin, or verapamil for 30 min. Then, they were washed and treated with calcein-AM for 30 min at 37 °C. The excitation and emission wavelengths were 485 and 528 nm, respectively. Using BioTek Synergy HT Multi-Mode Microplate Reader, fluorescence levels due to intracellular calcein were measured at 37 °C every 3 min for 30 min.

4.6. Rhodamine 123 and Doxorubicin Efflux Assays

The densities of ABCB1/Flp-InTM-293 and Flp-InTM-293 cells in 96-well plates were 1×10^5 and 1.4×10^5 cells/well, respectively. After 24 h of incubation, the cells were treated with pinostrobin or tectochrysin for 30 min. Then, they were incubated at 37 °C with rhodamine 123 for 30 min or doxorubicin for 1.5 h. Next, warm PBS was used to wash the cells, which were incubated for 10 and 25 min, respectively. The supernatant was added to 96-well black plates. A SpectraMax iD3 Multi-Mode Microplate Reader (Molecular Devices, San Jose, CA, USA) was used to measure fluorescence levels without light exposure. The excitation and emission wavelengths for rhodamine 123 were 485 and 528 nm, respectively; the corresponding wavelengths for doxorubicin were 485 and 590 nm, respectively.

4.7. MDR1 Shift Assay

Conformational changes in human P-gp were investigated by performing an MDR1 shift assay (MDR1 Shift Assay Kit; EMD Millipore Corp., Billerica, MA, USA). UIC2 antibodies can serve as conformation-sensitive antibodies against human MDR1. Upon the attachment of a substrate to P-gp, UIC2 binds to the open conformation of P-gp. For the assay, the cells were first treated with vinblastine (positive control), DMSO (solvent control), pinostrobin, or tectochrysin for 30 min. Then, they were incubated with the working solution of UIC2 or IgG2a (negative control antibody) for 15 min at 37 °C. After centrifugation at $200 \times g$ for 10 min, Alexa Fluor[®] 488 (MDR1 Shift Assay Kit; EMD Millipore Corp., Billerica, MA, USA)—a secondary antibody of UIC2—was incubated with the cells for 15 min at 4 °C. FACS analysis (BD FACSCantoTM II System) (BD, Franklin Lakes, NJ, USA) was performed to measure fluorescence levels.

4.8. P-gp ATPase Activity Assay

A Pgp-GloTM assay (Promega, Madison, WI, USA) was performed to assess the effects of pinostrobin or tectochrysin on the activity of P-gp ATPase. A series of test compound concentrations was added into 96-well white plates, followed by the addition of recombinant human P-gp membranes; the mixture was incubated for 5 min at 37 °C. Verapamil was used as a positive control. Then, the cells were incubated with MgATP for 80 min at 37 °C to induce P-gp ATPase activity. To stop the reaction, the mixture was incubated with ATPase Detection Reagent for 20 min at 26 °C. SpectraMax iD3 Multi-Mode Microplate Reader was used to detect luminescence. Changes in luminescence (ΔRLU) were recorded.

4.9. Cell Cycle Analysis

Cancer cells were incubated with serum-free medium in 6-well plates for 24 h at 37 °C. Then, the cells were incubated with chemotherapeutic drugs or their combinations with different concentrations of test compounds for 48 h at 37 °C. After harvesting and washing (cold PBS), the cells were incubated with 70% ethanol for at least 24 h for cellular fixation. After fixation, the cells were washed again with PBS and resuspended in staining buffer (FBS). Propidium iodide (PI)/RNase Staining Buffer (500 μ L; BD PharmingenTM, San Diego, CA, USA) was added to the cells, and the mixture was incubated for 15 min at room temperature under dark conditions. FACS analysis (BD FACSCantoTM II System) was performed to analyze the harvested cells. The excitation and emission wavelengths for PI were 488 and 575 nm, respectively. ModFit LT software is a flow cytometry analysis software. This software was used for DNA analysis to quantify cell cycle. The raw data were imported after open the software. First, the gate parameter and region would be

defined and enabled gate 1 to get the right peak distribution. Then, properties about debris, aggregates, and apoptosis were edited for manual analysis. Finally, the ranges of different cell phases would be regulated and fitted the selected peaks. The percent of each phase in cell cycle would be produced and used to be calculated.

4.10. Apoptosis Assay

The pattern of cell death was investigated using Annexin V-FITC/PI Apoptosis Detection Kit (Elabscience[®], Houston, TX, USA). The cells in 6-well plates were treated with chemotherapeutic drugs with or without the test compounds at 37 °C for 48 h. Subsequently, they were harvested and washed with cold PBS and resuspended in Annexin V Binding Buffer (1×; 500 mL). Subsequently, 5 µL of Annexin V-FITC or PI solution was added to 100 µL of the aforementioned suspension and incubated for 15 min at room temperature under dark conditions. Then, 400 µL 1× Binding Buffer was added to each mixture, which was then subjected to FACS analysis (BD FACSCanto[™] System). The excitation wavelength was 488 nm; the emission wavelengths for FITC and PI were 530 and 575 nm, respectively.

4.11. Western Blotting

Protein expression was assessed through Western blotting. KB and KBvin cells were plated in 6-well plates and treated with different concentrations of the test compounds for 48 h. The harvested cells were lysed in radioimmunoprecipitation assay buffer for 5 min at 4 °C. The suspensions were heated at 70 °C for 10 min and separated through sodium dodecyl sulfate–polyacrylamide gel electrophoresis. Subsequently, the separated bands on gels were transferred onto nitrocellulose membranes. The membranes were blocked with 5% nonfat milk for 1 h and incubated with antibodies for β-actin and P-gp at 4 °C overnight. Then, the blots were incubated with secondary antibodies for 1 h at 4 °C, followed by incubation with electrochemiluminescence reagent for 5 min at room temperature. Chemiluminescence levels were measured using Cytiva ImageQuant[™] 800 (Cytiva, Marlborough, MA, USA). Data were analyzed using Image Lab (version 6.0).

4.12. Molecular Docking

AutoDock (version 4.2.6) was used to simulate molecular docking, calculate the lowest binding energy, and identify the best binding site. The crystal structure of human P-gp (Protein Data Bank [PDB] ID: 7A65) [32] was downloaded from the Research Collaboratory for Structural Bioinformatics PDB. Ligand docking at the binding sites of P-gp was simulated using the standard procedure. A grid box (size, 70 Å × 70 Å × 70 Å) was centered at the coordinates 164.072 (*x*-axis), 157.954 (*y*-axis), and 159.047 (*z*-axis) of the PDB structure; 0.500 spacing was ensured. The population size was 300, and the number of genetic algorithm run was 50. LigPlus (version 2.2.4) was used to generate two-dimensional plots. The data were used to perform energy-based measurements and visualize and classify drug interactions.

4.13. Statistical Analysis

Student's *t*-tests were performed to determine statistical differences. Statistical significance was set at $p < 0.05$.

Supplementary Materials: The following supporting information can be downloaded at: <https://www.mdpi.com/article/10.3390/ph16020205/s1>, Figure S1: The distribution of CFSE fluorescence was analyzed by flow cytometry at 0, 24, 48 and 72 h; Figure S2: The raw data of Western blotting. Tables S1 and S2: IC₅₀ values (72 h) of only and the combination of tariquidar with paclitaxel in HeLa S3 and KBvin cells.

Author Contributions: I.-T.W. and C.-Y.K.: Conceptualization, data curation, formal analysis, methodology, validation, writing—original draft, writing—review and editing. C.-H.S. and Y.-H.L.: data curation, formal analysis, investigation, writing—review and editing. C.-C.H.: Conceptualization, data curation, supervision, methodology, validation, funding acquisition, project administration, resources, writing—original draft, writing—review and editing. All authors have read and agreed to the published version of the manuscript.

Funding: This research was funded by the China Medical University [CMU111-MF-23] and the Ministry of Science and Technology [MOST 111-2320-B-039-049 and 109-2320-B-303-004-MY3].

Institutional Review Board Statement: Not applicable.

Informed Consent Statement: Not applicable.

Data Availability Statement: Data is contained within the article and supplementary material.

Acknowledgments: Flow cytometry analyses were conducted at the Medical Research Core Facilities Center, Office of Research and Development at China Medical University, Taichung, Taiwan, R.O.C. We would like to acknowledge Kazumitsu Ueda (Kyoto University) and Kuo-Hsiung Lee (University of North Carolina, Chapel Hill) for providing the human MDR1 cDNA and the multidrug-resistant human cervical cancer cell line KB/VIN, respectively. This manuscript was edited by Wallace Academic Editing.

Conflicts of Interest: The authors declare no conflict of interest.

References

1. Bukowski, K.; Kciuk, M.; Kontek, R. Mechanisms of Multidrug Resistance in Cancer Chemotherapy. *Int. J. Mol. Sci.* **2020**, *21*, 3233. [[CrossRef](#)] [[PubMed](#)]
2. Binkhathlan, Z.; Lavasanifar, A. P-glycoprotein inhibition as a therapeutic approach for overcoming multidrug resistance in cancer: Current status and future perspectives. *Curr. Cancer Drug Targets* **2013**, *13*, 326–346. [[CrossRef](#)] [[PubMed](#)]
3. Amawi, H.; Sim, H.M.; Tiwari, A.K.; Ambudkar, S.V.; Shukla, S. ABC Transporter-Mediated Multidrug-Resistant Cancer. *Adv. Exp. Med. Biol.* **2019**, *1141*, 549–580. [[CrossRef](#)] [[PubMed](#)]
4. Leith, C.P.; Kopecky, K.J.; Chen, I.M.; Eijdem, L.; Slovak, M.L.; McConnell, T.S.; Head, D.R.; Weick, J.; Grever, M.R.; Appelbaum, F.R.; et al. Frequency and clinical significance of the expression of the multidrug resistance proteins MDR1/P-glycoprotein, MRP1, and LRP in acute myeloid leukemia: A Southwest Oncology Group Study. *Blood* **1999**, *94*, 1086–1099. [[PubMed](#)]
5. Mechetner, E.; Kyshtoobayeva, A.; Zonis, S.; Kim, H.; Stroup, R.; Garcia, R.; Parker, R.J.; Fruehauf, J.P. Levels of multidrug resistance (MDR1) P-glycoprotein expression by human breast cancer correlate with in vitro resistance to taxol and doxorubicin. *Clin. Cancer Res.* **1998**, *4*, 389–398.
6. Huang, C.Y.; Ju, D.T.; Chang, C.F.; Muralidhar Reddy, P.; Velmurugan, B.K. A review on the effects of current chemotherapy drugs and natural agents in treating non-small cell lung cancer. *BioMedicine* **2017**, *7*, 23. [[CrossRef](#)] [[PubMed](#)]
7. Tinoush, B.; Shirdel, I.; Wink, M. Phytochemicals: Potential Lead Molecules for MDR Reversal. *Front. Pharmacol.* **2020**, *11*, 832. [[CrossRef](#)]
8. Ghaffari, T.; Hong, J.H.; Asnaashari, S.; Farajnia, S.; Delazar, A.; Hamishehkar, H.; Kim, K.H. Natural Phytochemicals Derived from Gymnosperms in the Prevention and Treatment of Cancers. *Int. J. Mol. Sci.* **2021**, *22*, 6636. [[CrossRef](#)]
9. Jones, A.A.; Gehler, S. Acacetin and Pinostrobin Inhibit Malignant Breast Epithelial Cell Adhesion and Focal Adhesion Formation to Attenuate Cell Migration. *Integr. Cancer* **2020**, *19*, 1534735420918945. [[CrossRef](#)]
10. Kuete, V.; Nkuete, A.H.; Mbaveng, A.T.; Wiench, B.; Wabo, H.K.; Tane, P.; Efferth, T. Cytotoxicity and modes of action of 4'-hydroxy-2',6'-dimethoxychalcone and other flavonoids toward drug-sensitive and multidrug-resistant cancer cell lines. *Phytomed.* *Int. J. Phytother. Phytopharm.* **2014**, *21*, 1651–1657. [[CrossRef](#)]
11. Patel, N.K.; Jaiswal, G.; Bhutani, K.K. A review on biological sources, chemistry and pharmacological activities of pinostrobin. *Nat. Prod. Res.* **2016**, *30*, 2017–2027. [[CrossRef](#)] [[PubMed](#)]
12. Park, M.H.; Hong, J.E.; Park, E.S.; Yoon, H.S.; Seo, D.W.; Hyun, B.K.; Han, S.B.; Ham, Y.W.; Hwang, B.Y.; Hong, J.T. Anticancer effect of tectochrysin in colon cancer cell via suppression of NF-kappaB activity and enhancement of death receptor expression. *Mol. Cancer* **2015**, *14*, 124. [[CrossRef](#)]
13. He, B.; Xu, F.; Yan, T.; Xiao, F.; Wu, B.; Wang, Y.; Bi, K.; Jia, Y. Tectochrysin from *Alpinia Oxyphylla* Miq. alleviates A β (1-42) induced learning and memory impairments in mice. *Eur. J. Pharm.* **2019**, *842*, 365–372. [[CrossRef](#)] [[PubMed](#)]
14. Park, M.H.; Hong, J.E.; Hwang, C.J.; Choi, M.; Choi, J.S.; An, Y.J.; Son, D.J.; Hong, J.T. Synergistic inhibitory effect of cetuximab and tectochrysin on human colon cancer cell growth via inhibition of EGFR signal. *Arch. Pharm. Res.* **2016**, *39*, 721–729. [[CrossRef](#)] [[PubMed](#)]

15. Ahmed-Belkacem, A.; Pozza, A.; Muñoz-Martínez, F.; Bates, S.E.; Castanys, S.; Gamarro, F.; Di Pietro, A.; Pérez-Victoria, J.M. Flavonoid structure-activity studies identify 6-prenylchrysin and tectochrysin as potent and specific inhibitors of breast cancer resistance protein ABCG2. *Cancer Res.* **2005**, *65*, 4852–4860. [[CrossRef](#)]
16. Mohana, S.; Ganesan, M.; Agilan, B.; Karthikeyan, R.; Srithar, G.; Beulah Mary, R.; Ananthkrishnan, D.; Velmurugan, D.; Rajendra Prasad, N.; Ambudkar, S.V. Screening dietary flavonoids for the reversal of P-glycoprotein-mediated multidrug resistance in cancer. *Mol. Biosyst.* **2016**, *12*, 2458–2470. [[CrossRef](#)]
17. Li, W.; Zhang, H.; Assaraf, Y.G.; Zhao, K.; Xu, X.; Xie, J.; Yang, D.H.; Chen, Z.S. Overcoming ABC transporter-mediated multidrug resistance: Molecular mechanisms and novel therapeutic drug strategies. *Drug Resist. Update* **2016**, *27*, 14–29. [[CrossRef](#)]
18. Robey, R.W.; Pluchino, K.M.; Hall, M.D.; Fojo, A.T.; Bates, S.E.; Gottesman, M.M. Revisiting the role of ABC transporters in multidrug-resistant cancer. *Nat. Rev. Cancer* **2018**, *18*, 452–464. [[CrossRef](#)]
19. Lai, J.I.; Tseng, Y.J.; Chen, M.H.; Huang, C.F.; Chang, P.M. Clinical Perspective of FDA Approved Drugs With P-Glycoprotein Inhibition Activities for Potential Cancer Therapeutics. *Front. Oncol.* **2020**, *10*, 561936. [[CrossRef](#)]
20. Pajic, M.; Iyer, J.K.; Kersbergen, A.; van der Burg, E.; Nygren, A.O.; Jonkers, J.; Borst, P.; Rottenberg, S. Moderate increase in Mdr1a/1b expression causes in vivo resistance to doxorubicin in a mouse model for hereditary breast cancer. *Cancer Res.* **2009**, *69*, 6396–6404. [[CrossRef](#)] [[PubMed](#)]
21. Kumar, A.; Jaitak, V. Natural products as multidrug resistance modulators in cancer. *Eur. J. Med. Chem.* **2019**, *176*, 268–291. [[CrossRef](#)] [[PubMed](#)]
22. Imai, Y.; Tsukahara, S.; Asada, S.; Sugimoto, Y. Phytoestrogens/flavonoids reverse breast cancer resistance protein/ABCG2-mediated multidrug resistance. *Cancer Res.* **2004**, *64*, 4346–4352. [[CrossRef](#)] [[PubMed](#)]
23. Chang, H.Y.; Pan, K.L.; Ma, F.C.; Jiao, X.Y.; Zhu, H.F.; Liu, J.H.; Huang, Y.; Cao, Y.H. The study on reversing mechanism of multidrug resistance of K562/A02 cell line by curcumin and erythromycin. *Zhonghua Xue Ye Xue Za Zhi = Zhonghua Xueyexue Zazhi* **2006**, *27*, 254–258. [[PubMed](#)]
24. Ganta, S.; Amiji, M. Coadministration of Paclitaxel and curcumin in nanoemulsion formulations to overcome multidrug resistance in tumor cells. *Mol. Pharm.* **2009**, *6*, 928–939. [[CrossRef](#)] [[PubMed](#)]
25. Lei, Y.; Tan, J.; Wink, M.; Ma, Y.; Li, N.; Su, G. An isoquinoline alkaloid from the Chinese herbal plant *Corydalis yanhusuo* W.T. Wang inhibits P-glycoprotein and multidrug resistance-associate protein 1. *Food Chem.* **2013**, *136*, 1117–1121. [[CrossRef](#)]
26. Ferreira, R.J.; Ferreira, M.J.; dos Santos, D.J. Molecular docking characterizes substrate-binding sites and efflux modulation mechanisms within P-glycoprotein. *J. Chem. Inf. Model* **2013**, *53*, 1747–1760. [[CrossRef](#)]
27. Abdelfatah, S.; Böckers, M.; Asensio, M.; Kadioglu, O.; Klinger, A.; Fleischer, E.; Efferth, T. Isopetasin and S-isopetasin as novel P-glycoprotein inhibitors against multidrug-resistant cancer cells. *Phytomed. Int. J. Phytother. Phytopharm.* **2021**, *86*, 153196. [[CrossRef](#)] [[PubMed](#)]
28. Borst, P. Looking back at multidrug resistance (MDR) research and ten mistakes to be avoided when writing about ABC transporters in MDR. *FEBS Lett.* **2020**, *594*, 4001–4011. [[CrossRef](#)]
29. Teng, Y.N.; Sheu, M.J.; Hsieh, Y.W.; Wang, R.Y.; Chiang, Y.C.; Hung, C.C. β -carotene reverses multidrug resistant cancer cells by selectively modulating human P-glycoprotein function. *Phytomed. Int. J. Phytother. Phytopharm.* **2016**, *23*, 316–323. [[CrossRef](#)]
30. Chou, T.C. Drug combination studies and their synergy quantification using the Chou-Talalay method. *Cancer Res.* **2010**, *70*, 440–446. [[CrossRef](#)]
31. Georgiou, M.; Ntavelou, P.; Stokes, W.; Roy, R.; Maher, G.J.; Stoilova, T.; Choo, J.; Rakhit, C.P.; Martins, M.; Ajuh, P.; et al. ATR and CDK4/6 inhibition target the growth of methotrexate-resistant choriocarcinoma. *Oncogene* **2022**, *41*, 2540–2554. [[CrossRef](#)] [[PubMed](#)]
32. Nosol, K.; Romane, K.; Irobalieva, R.N.; Alam, A.; Kowal, J.; Fujita, N.; Locher, K.P. Cryo-EM structures reveal distinct mechanisms of inhibition of the human multidrug transporter ABCB1. *Proc. Natl. Acad. Sci. USA* **2020**, *117*, 26245–26253. [[CrossRef](#)] [[PubMed](#)]

Disclaimer/Publisher’s Note: The statements, opinions and data contained in all publications are solely those of the individual author(s) and contributor(s) and not of MDPI and/or the editor(s). MDPI and/or the editor(s) disclaim responsibility for any injury to people or property resulting from any ideas, methods, instructions or products referred to in the content.